Superconducting properties of the attractive Hubbard model: A slave-boson study

Bogdan R. Bułka*
Institute of Molecular Physics, Polish Academy of Sciences, Smoluchowskiego 17, 60-179 Poznań, Poland

Stanisław Robaszkiewicz†
Department of Physics, A. Mickiewicz University, Umultowska 85, 61-614 Poznań, Poland
(Received 22 July 1996)

The superfluid characteristics of the attractive Hubbard model are analyzed for any coupling $|U|$ and arbitrary electron concentration $(0<n<2)$ by means of the slave-boson mean-field method and also by the perturbative treatment of the strong-coupling limit. The slave boson method takes into account correlations of electrons and yields a reliable description of the crossover from BCS-type superconductivity to local pair (composite bosons) superconductivity with increasing $|U|$. The results for the ground state (the free energy, the gap in the excitation spectrum) and the electromagnetic characteristics (the critical magnetic field, the London penetration depth, the coherence length) are compared with those obtained by the Hartree-Fock approximation and by the self-consistent second-order perturbation theory in the weak-coupling limit as well as with those obtained using perturbational approaches in the strong-coupling limit. We show that the slave-boson method, in contrast to the Hartree-Fock approximation, gives credible results for all investigated quantities in the whole interaction range, interpolating smoothly between the BCS and local pair regimes. A comparison of theoretical predictions for our simple model with experimental data for various families of short-coherence-length superconductors suggests that the best agreement can be obtained for intermediate values of the local attraction. [S0163-1829(96)05942-5]

I. INTRODUCTION

One of the conceptually simplest models for studying correlations and to describe the superconductivity of the systems with short-range, almost unretarded pairing is the attractive Hubbard model.[1] It constitutes a common basis for the description of superconductors with weak local electron pairing, being in many ways similar to the conventional BCS systems and systems with a strong attraction, where superconductivity results from the condensation of hard-core composite charged bosons and is similar to the superfluidity of ^{4}He II. Such a model has been considered as an effective model of superconductivity in the family of cuprates,[2,3] the barium bismuthates ($Ba_{1-x}K_xBiO_3$ and $BaPb_xBi_{1-x}O_3$),[1,4] and the fullerides,[5] as well as the Chevrel phases.[1]

In this paper we study the basic superfluid characteristics of this model by means of the slave-boson (mean-field) theory and also by the perturbative treatment of the strong-coupling limit, where one is able to get several rigorous results for three-dimensional (3D) lattices using a systematic low-density expansion based on knowledge of the exact two-body scattering amplitude. The slave-boson method is in principle not restricted to weak or strong coupling. It is an improvement over the Hartree-Fock approximation (HFA) since it takes local correlations into account; in particular, the density of doubly occupied lattice sites is an independent parameter to be optimized. In fact, it was shown[6] that the slave-boson mean-field approximation (SBMFA) is equivalent to the Gutzwiller approximation to the Gutzwiller wave function.[7] Although the repulsive Hubbard model and its various generalizations have been extensively analyzed by this approach,[8,9] for the attractive case the method has only been used in the works of Sofo and Balseiro[10] and Bułka.[11] The main purpose of our work is to extend those investigations and to discuss also the electromagnetic properties of the model. We perform the calculations of the energy gap E_g, the London penetration depth λ, the thermodynamic critical field H_c, and the Ginzburg-Landau correlation length ξ_{GL} and analyze the evolution of these quantities as a function of electron concentration n and the increasing interaction U. Several analytical results concerning the ground-state characteristics, which can be derived in both the weak-coupling and strong-coupling limits, are also presented for comparison with numerical solutions and with the results of other approaches.

The paper is organized as follows. In the next section we briefly introduce the spin- and charge-rotationally invariant slave-boson representation for the considered model. We present the free energies for the superconducting and the normal phases as well as the corresponding consistency equations derived within the SBMFA, and analyze the behavior of the ground-state energy, the chemical potential, and the energy gap in the quasiparticle excitation spectrum. In Sec. III the electromagnetic properties of the model are studied within the SBMFA and their evolution with increasing interaction and electron concentration is discussed. In Sec. IV we present the results for the strong attraction limit of the model obtained using the effective pseudospin model and compare them with those of the SBMFA. The last section is devoted to conclusions and a supplementary discussion including some comparisons of theoretical predictions with experimental results for various families of short-coherence-length superconductors. In Appendix A the SBMFA solutions for the normal state are given, whereas Appendix B summarizes the analytical results for the

ground-state characteristics which can be derived in the limit of weak coupling within the SBMFA and HFA.

II. CHARACTERISTICS OF THE GROUND STATE

A. Description of the Hubbard model in the spin- and charge-rotationally invariant slave-boson representation

In this section we want to present the slave-boson representation of electronic operators, which is the spin- and charge-rotationally invariant. The method allows us to investigate various magnetic orderings as well as the superconducting and charge ordered phases. We follow the procedure described in Refs. 12 and 11. The singly occupied states $|\sigma\rangle$ are expressed by the Bose operators $p^{\dagger}_{\sigma\sigma'}$ and the Fermi operators $f^{\dagger}_{\sigma}$ as

$$|\sigma\rangle=\sum_{\sigma'} p^{\dagger}_{\sigma\sigma'}f^{\dagger}_{\sigma'}|\mathrm{vac}\rangle \quad (\sigma=+,-). \tag{1}$$

The site index is omitted for clarity. The doubly occupied state $|2\rangle$ and the state $|0\rangle$, corresponding to an empty site, form a doublet $|\rho\rangle$ $(\rho=+,-)$, which may be expressed by the Bose operators $b^{\dagger}_{\rho\rho'}$ as

$$|\rho\rangle=\sum_{\rho'} b^{\dagger}_{\rho\rho'}\psi^{\dagger}_{\rho'}|\mathrm{vac}\rangle, \tag{2}$$

where

$$\psi^{\dagger}_{\rho}=\begin{pmatrix} f^{\dagger}_{+}f^{\dagger}_{-} \\ 1 \end{pmatrix}. \tag{3}$$

The operators $b_{\rho\rho'}$ and $p_{\sigma\sigma'}$ obey the commutation relations

$$[b_{\rho_1\rho_2},b^{\dagger}_{\rho_3\rho_4}]=\frac{1}{2}\delta_{\rho_1\rho_4}\delta_{\rho_2\rho_3},$$

$$[p_{\sigma_1\sigma_2},p^{\dagger}_{\sigma_3\sigma_4}]=\frac{1}{2}\delta_{\sigma_1\sigma_4}\delta_{\sigma_2\sigma_3}. \tag{4}$$

In order to operate in the physical part of the extended Hilbert space we introduce the following constraint:

$$2\sum_{\rho\rho'} b^{\dagger}_{\rho\rho'}b_{\rho'\rho}+2\sum_{\sigma\sigma'} p^{\dagger}_{\sigma\sigma'}p_{\sigma'\sigma}=1. \tag{5}$$

It ensures that each site is occupied by exactly one slave boson. The electron creation operator $c^{\dagger}_{\sigma}$ is expressed by

$$c^{\dagger}_{\sigma}\equiv|\sigma\rangle\langle 0|+\sigma|2\rangle\langle\sigma|=\sum_{\sigma'}(z^{\dagger}_{+\sigma,+\sigma'}f^{\dagger}_{\sigma'}+\sigma' z^{\dagger}_{+\sigma,-\sigma'}f_{\sigma'}), \tag{6}$$

where

$$z^{\dagger}_{+\sigma,+\sigma'}=p^{\dagger}_{\sigma'\sigma}\tilde{b}_{++}+b^{\dagger}_{++}\tilde{p}_{\sigma'\sigma},$$

$$z^{\dagger}_{+\sigma,-\sigma'}=p^{\dagger}_{\sigma'\sigma}\tilde{b}_{+-}+b^{\dagger}_{+-}\tilde{p}_{\sigma'\sigma}. \tag{7}$$

$\tilde{b}_{\rho\rho'}$ and $\tilde{p}_{\sigma\sigma'}$ are the time-reversed operators of $b_{\rho\rho'}$ and $p_{\sigma\sigma'}$ (i.e., $\tilde{b}_{\rho\rho'}=\rho\rho' b_{\overline{\rho'}\overline{\rho}}$ and $\tilde{p}_{\sigma\sigma'}=\sigma\sigma' p_{\overline{\sigma'}\overline{\sigma}}$). The physical variable may be expressed by the slave bosons in the following form: the spin operator by

$$\mathbf{S}=\sum_{\sigma\sigma'} c^{\dagger}_{\sigma}\tau_{\sigma\sigma'}c_{\sigma'}=\sum_{\sigma\sigma'\sigma''}\tau_{\sigma\sigma'}p^{\dagger}_{\sigma\sigma'}p_{\sigma'\sigma''}, \tag{8}$$

analogously, the operator $\mathbf{J}$ [defined as $J^{+}=c^{\dagger}_{+}c^{\dagger}_{-}$, $J^{-}=c_{-}c_{+}$, $J^{z}=\frac{1}{2}(c^{\dagger}_{+}c_{+}+c^{\dagger}_{-}c_{-}-1)$] by

$$\mathbf{J}=\sum_{\rho\rho'\rho''}\tau_{\rho\rho'}b^{\dagger}_{\rho\rho'}b_{\rho'\rho''}, \tag{9}$$

the number of electrons with spin σ by

$$n_{\sigma}=\frac{1}{2}+J^{z}+\sigma S^{z}, \tag{10}$$

and the operator of a doubly occupied site $D=n_{+}n_{-}$ by

$$D=2\sum_{\rho} b^{\dagger}_{+\rho}b_{\rho+}. \tag{11}$$

Additionally one finds the relations

$$f^{\dagger}_{\sigma}f_{\sigma'}=2\sum_{\sigma_1} p^{\dagger}_{\sigma_1\sigma}p_{\sigma'\sigma_1}+2\delta_{\sigma'\sigma}\sum_{\rho} b^{\dagger}_{\rho+}b_{+\rho}, \tag{12}$$

$$f^{\dagger}_{+}f^{\dagger}_{-}=2\sum_{\rho} b^{\dagger}_{\rho-}b_{+\rho} \quad \text{and} \quad f_{-}f_{+}=2\sum_{\rho} b^{\dagger}_{\rho+}b_{-\rho}. \tag{13}$$

Using the above relations [Eqs. (5–13)] one can express the Hubbard Hamiltonian

$$H=t\sum_{ij,\sigma}{}' (c^{\dagger}_{i\sigma}c_{j\sigma}+\mathrm{H.c.})-\mu\sum_{i,\sigma} c^{\dagger}_{i\sigma}c_{i\sigma}+U\sum_{i} n_{i+}n_{i-} \tag{14}$$

in the slave-boson representation as

$$H=t\sum_{ij}{}'\sum_{\sigma'\sigma''}[q_{ij,\sigma'\sigma''}f^{\dagger}_{i\sigma'}f_{j\sigma''}+r_{ij,\sigma'\sigma''}f_{i-\sigma'}f_{j\sigma''}+\mathrm{H.c.}]$$

$$-\mu\sum_{i}(2J^{z}_{i}+1)+2U\sum_{i,\rho} b^{\dagger}_{i+\rho}b_{i\rho+}, \tag{15}$$

where

$$q_{ij,\sigma'\sigma''}=\sum_{\sigma}(\tilde{z}^{\dagger}_{i+\sigma,+\sigma'}\tilde{z}_{j+\sigma,+\sigma''}-\sigma'\sigma''\tilde{z}^{\dagger}_{j+\sigma,-\overline{\sigma''}}\tilde{z}_{i+\sigma,-\overline{\sigma'}}), \tag{16}$$

$$r_{ij,\sigma'\sigma''}=\sigma'\sum_{\sigma}\tilde{z}^{\dagger}_{i+\sigma,-\sigma'}\tilde{z}_{j+\sigma,+\sigma''}. \tag{17}$$

Σ' denotes a summation confined to nearest-neighbor sites. The operators $\tilde{z}$ are those from Eq. (7) properly renormalized to get the correct result in the noninteracting limit $(U\rightarrow 0)$.[6,11,12] In our case they are

$$\underline{\tilde{z}}=\underline{\tilde{b}}^{\dagger}\underline{\underline{LR}}\underline{p}+\underline{\tilde{p}}^{\dagger}\underline{\underline{LR}}\underline{b}, \tag{18}$$

where

$$\underline{L}=[\underline{1}-2\underline{b}^{\dagger}\underline{b}-2\underline{p}^{\dagger}\underline{p}]^{-1/2},\underline{R}=[\underline{1}-2\underline{\tilde{b}}^{\dagger}\underline{\tilde{b}}-2\underline{\tilde{p}}^{\dagger}\underline{\tilde{p}}]^{-1/2}. \tag{19}$$

An underbar denotes the 2×2 matrix.

B. Properties of the mean-field ground state

Now we want to find stable mean-field solutions for the slave-boson Hamiltonian (15). We investigate the normal (N) and the superconducting state (S) for any electron concentration n and any negative value of U. We will not present the solutions for the charge density wave (CDW) state. Such solutions do exist in a definite range of U/t and n, but except for $n=1$ their free energy is always higher than that of S. The superconducting order parameter can be defined using the operator J^{-} [Eq. (9)] as

$$\Delta_i\equiv\langle c_{i-}c_{i+}\rangle=2\sum_{\rho}\langle b^{\dagger}_{i\rho+}b_{i-\rho}\rangle. \tag{20}$$

Assuming a uniform superconducting state and the absence of magnetic ordering one has $\Delta=2\langle b^{\dagger}_{i++}b_{i-+}+b^{\dagger}_{i-+}b_{i--}\rangle$, $\langle p_{i++}\rangle=\langle p_{i--}\rangle$, and $\langle p_{i+-}\rangle=\langle p_{i-+}\rangle=0$. Taking $b^2=2\langle b^{\dagger}_{i++}b_{i++}+b^{\dagger}_{i--}b_{i--}+b^{\dagger}_{i+-}b_{i-+}+b^{\dagger}_{i-+}b_{i+-}\rangle$, $p^2=2\langle p^{\dagger}_{i++}p_{i++}+p^{\dagger}_{i--}p_{i--}\rangle$, and $\delta=\langle b^{\dagger}_{i++}b_{i++}-b^{\dagger}_{i--}b_{i--}\rangle$, one gets the hopping factors [Eqs. (16) and (17)] as

$$q_S=\langle q_{ij,\sigma\sigma}\rangle=\{p^2[(b^2+2\delta+2\Delta)^{1/2}+(b^2-2\delta-2\Delta)^{1/2}]^2\}/\{1-4\delta^2-4\Delta^2\}, \tag{21}$$

and $r=\langle r_{ij,\sigma'\sigma''}\rangle=0$. The constraints imposed by Eqs. (5) and (8)–(13) are introduced to the partition function with Lagrange multiplier fields. The number of Lagrange multipliers can be easily reduced; in particular, condition (5) means $p^2+b^2=1$ and from Eq. (10) the electron concentration $n=1+2\delta$. We assume all Lagrange multiplier fields as space and time independent. The ground state is determined from a saddle point of the partition function, i.e., from the minimum of the free energy F with respect to the variables p, b, δ, and Δ. The free energy is the sum of the fermionic and the bosonic parts $F=F_f+F_b$, which are given by

$$F_f/N=-\frac{1}{N\beta}\sum_{\mathbf{k}}[\ln\{1+\exp(\beta E_{\mathbf{k}})\}+\ln\{1+\exp(-\beta E_{\mathbf{k}})\}], \tag{22}$$

$$F_b/N=-\frac{|U|}{2}(b^2+2\delta)-(\lambda_1+\mu)(1+2\delta)-2\lambda_S\Delta. \tag{23}$$

Here, N denotes the number of the lattice sites, $E_{\mathbf{k}}=[(q_S\epsilon_{\mathbf{k}}+\lambda_1)^2+\lambda_S^2]^{1/2}$, λ_1 and λ_S are the Lagrange multipliers for the constraints (12) and (13), and $\epsilon_{\mathbf{k}}$ is the energy dispersion of noninteracting electrons. The minimum of F is determined by

$$\frac{1}{N}\frac{\partial F}{\partial\lambda_1}=\frac{1}{N}\frac{\partial F_f}{\partial\lambda_1}-(1+2\delta)=0, \tag{24}$$

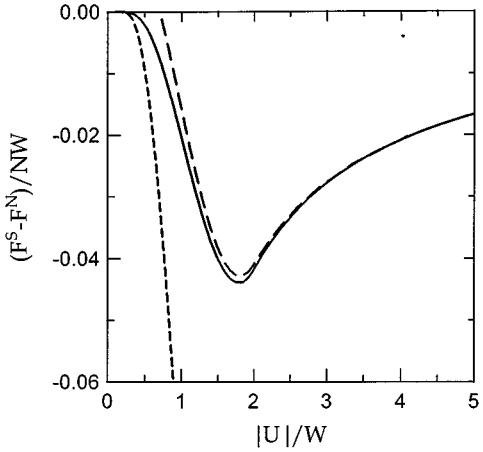

FIG. 1. Free energy difference of the superconducting and the normal state calculated within the SBMFA (solid curve) at $n=1$. For comparison, the corresponding Hartree-Fock result is shown by the short-dashed curve and the difference of the free energy of the superconducting state in the Hartree-Fock approximation and the normal state in the slave-boson approach ($F^S_{\mathrm{HF}}-F^N_{\mathrm{sb}}$) by the long-dashed curve.

$$\frac{1}{N}\frac{\partial F}{\partial b}=\frac{1}{N}\frac{\partial F_f}{\partial q_S}\frac{\partial q_S}{\partial b}-|U|b=0, \tag{25}$$

$$\frac{1}{N}\frac{\partial F}{\partial\lambda_S}=\frac{1}{N}\frac{\partial F_f}{\partial\lambda_S}-2\Delta=0, \tag{26}$$

$$\frac{1}{N}\frac{\partial F}{\partial\Delta}=\frac{1}{N}\frac{\partial F_f}{\partial q_S}\frac{\partial q_S}{\partial\Delta}-2\lambda_S=0. \tag{27}$$

In our derivations we will mainly use the rectangular density of states $\rho(\epsilon)=1/W$ for $|\epsilon|\leq W/2$, where W is the width of the electronic band. We restrict our considerations to the case of $T=0$. The fermionic part of the free energy of the superconducting phase at $T=0$ is

$$F^S_f/N=\lambda_1-\frac{q_SW}{8}\left\{(R_++R_-)+\overline{\lambda_1}(R_+-R_-)+\overline{\lambda_S^2}\ln\frac{R_++\overline{\lambda_1}+1}{R_-+\overline{\lambda_1}-1}\right\}, \tag{28}$$

where $\overline{\lambda_\alpha}=2\lambda_\alpha/q_SW$ $(\alpha=1,S)$ and $R_\pm=[(\overline{\lambda_1}\pm1)^2+\overline{\lambda_S^2}]^{1/2}$. For the normal state $(\Delta=0)$ the solutions are given in a parametric way in Appendix A.

In general Eqs. (24)–(27) can be solved numerically. The results are presented in Figs. 1–6. The difference of the free energy of the superconducting state and the normal state ΔF is exhibited in Fig. 1 for $n=1$ (solid curve). For comparison the Hartree-Fock solution for the Hubbard Hamiltonian (14) is[13,14]

$$F^N_{\mathrm{HF}}/N=-\frac{W}{4}n(2-n)-\frac{|U|}{4}n^2, \tag{29}$$

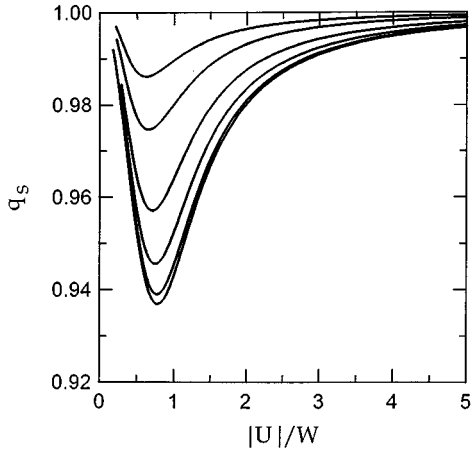

FIG. 2. Band narrowing factor q_S for the superconducting state vs the interaction parameter $|U|$ for the electron concentration $n=1$, 0.8, 0.6, 0.4, 0.2, and 0.1, from the bottom.

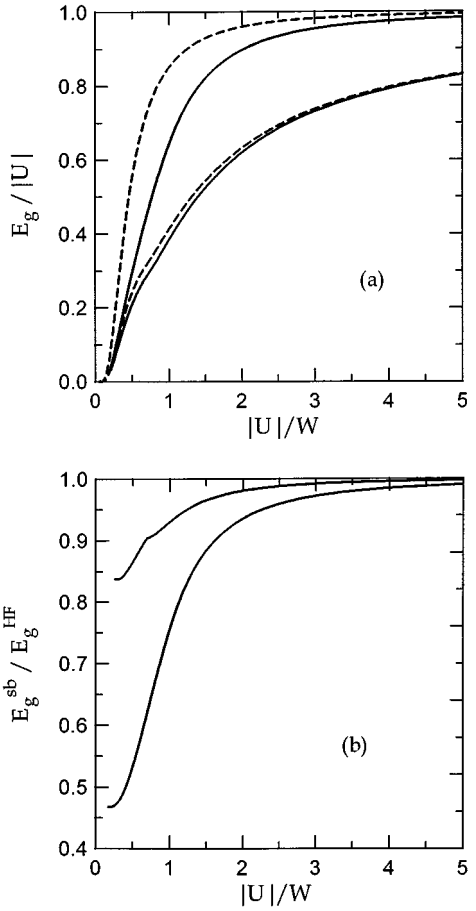

FIG. 3. The gap in the excitation spectrum E_g vs $|U|$ (a) for the electron concentration $n=1$ and 0.1 (from top) calculated within the SBMFA (solid curve) and the HFA (dashed curve). (b) shows the ratio of the energy gaps obtained by the slave-boson and HF methods, E_g^{sb}/E_g^{HF}, as a function of $|U|$ (from bottom for $n=1$ and 0.1).

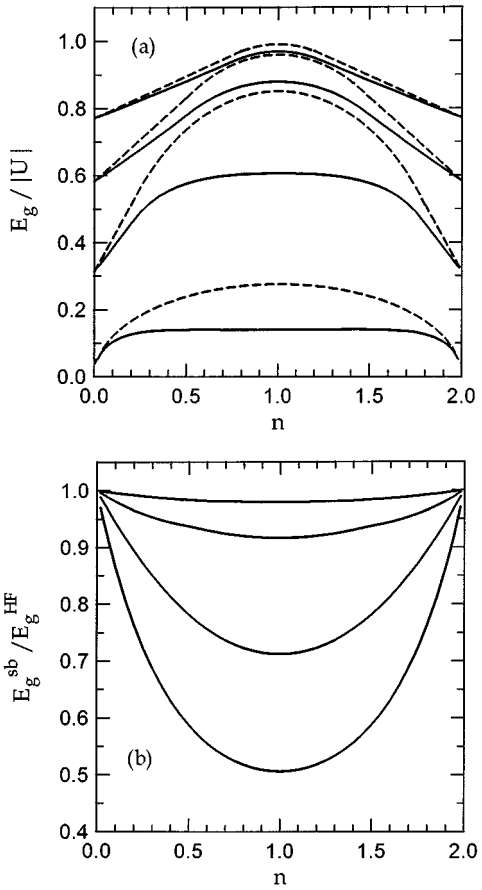

FIG. 4. The gap E_g as a function of n (a) for $|U|=4W$, $2W$, W, and $0.5W$ (from top) for the SBMFA (solid curve) and the HFA (dashed curve). (b) shows the ratio of E_g obtained by the SBMFA and the HFA (from top for $|U|=4W$, $2W$, W, and $0.5W$).

$$F_{\mathrm{HF}}^{S}/N=-\frac{W}{4}n(2-n)\coth\left(\frac{W}{|U|}\right)-\frac{|U|}{4}n^2, \qquad (30)$$

for the normal and the superconducting states, respectively. In this approach also the rectangular density of state is assumed. The difference $F_{\mathrm{HF}}^{S}-F_{\mathrm{HF}}^{N}$ is shown in Fig. 1 by the

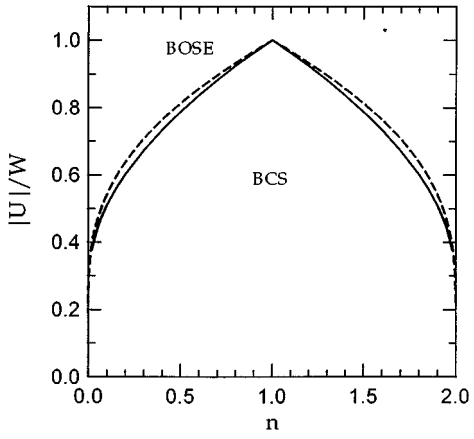

FIG. 5. Borderline between the region of the BCS-like and the local pair superconductivity obtained by the SBMFA (solid curve) and the HFA (dashed curve).

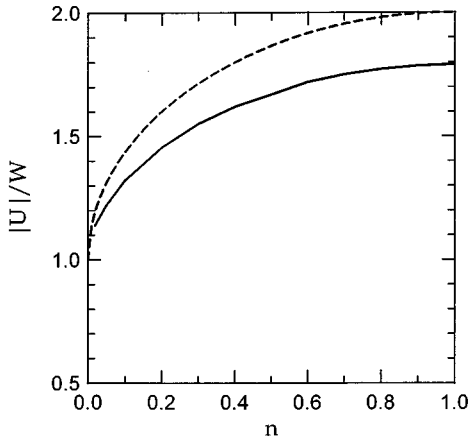

FIG. 6. Position of the maximum of the absolute value of the difference of the free energy of the superconducting and the normal states as a function of the electron concentration n (solid curve). The dashed curve represents the critical value of $|U_c|$, at which the bandwidth in the normal state is reduced to zero ($q_N=0$) (see Appendix A).

short-dashed curve. The expansion of the free energy for the slave-boson approach as well as the Hartree-Fock solution in the limit $|U|\to 0$ gives the ratio of the free energy differences $\gamma^2\equiv|\Delta F|/|\Delta F_{\rm HF}|=e^{-3/2}\simeq 0.22$ (see Appendix B). This value holds in a wide range of $|U|$. For larger values of $|U|>W$ there are great differences in the ΔF and the $\Delta F_{\rm HF}$ (although the free energies of the superconducting state for both type approximations are relatively close to each other). This is due to neglect of the effects of electron correlations in the normal state by the HFA. The crucial role of the correlation effects in the normal state in determining of the condensation energy ΔF is seen from the plot $F^S_{\rm HF}-F^N$ (long-dashed curve in Fig. 1).

Figure 2 represents the $|U|$ dependence of the band-narrowing factor q_S in the superconducting phase for different electron concentrations n. In contrast to the situation in the normal phase, where the changes of q_N are serious (see Appendix A), in the superconducting phase q_S is close to unity. However, these minor changes are relevant for the stability of superconductivity in the weak and intermediate regions of $|U|$ (i.e., for $|U|<2W$) and for the deviation of the slave-boson superconducting solutions from the results of the HFA.

The energy gap E_g in the excitation spectrum in the superconducting state ($T=0$) is given by $E_g=2\,\min(E_{\mathbf{k}})$, where the dispersion $E_{\mathbf{k}}=\sqrt{(q_S\epsilon_{\mathbf{k}}+\lambda_1)^2+\lambda_S^2}$. In Fig. 3(a) we show E_g vs $|U|$ (solid curve) for two electron concentrations $n=1$ and 0.1. For comparison the HF solution is[1,15]

$$E_g^{\rm HF}=2|U|\Delta_{\rm HF}\quad \text{for}\ \ |\overline{\mu}|<W/2,$$
$$E_g^{\rm HF}=2\sqrt{(W/2-|\overline{\mu}|)^2+|U|^2\Delta_{\rm HF}^2}\quad \text{for}\ \ |\overline{\mu}|>W/2, \tag{31}$$

where

$$\Delta_{\rm HF}=\frac{W}{2|U|}\sqrt{n(2-n)}/\sinh(W/|U|)$$

and

$$\overline{\mu}=\frac{W}{2}(n-1)\coth(W/|U|).$$

This is represented in Fig. 3(a) as the dashed curve. The ratio of E_g obtained for these two approaches is given in Fig. 3(b). For small $|U|$ and $n=1$ this ratio is equal to $\gamma=\exp(-3/4)\simeq 0.47$ (see also Appendix B for an analytical derivation). With the increasing interaction $|U|$, γ increases and E_g becomes closer to that one predicted in the HFA. The role of correlations decreases with decreasing number of electrons [see the case $n=0.1$ in Fig. 3(b)]. The dependence of the excitation gap E_g on the electron concentration for different values of $|U|$ is presented in Fig. 4(a). In the limit $n\to 0$ (or $n\to 2$) the both solutions goes to the exact result for the binding energy of the single Cooper pair in an empty lattice (Ref. 1), $E_b=2W/[\exp(2W/|U|)-1]$. The dependence of the ratio of E_g on n is presented in Fig. 4(b). Once again we see that the local correlation effects in the superconducting phase are most significant for E_g at n close to 1 and small $|U|$.

Using the SBMFA we can analyze the crossover from BCS-like superconductivity, with extended Cooper pairs, to superconductivity of composite bosons (local Cooper pairs), which occurs when one goes from a weak- to strong-coupling regime (from $|U|\ll W$ to $|U|\gg W$). At $T=0$ the approximate boundary between both regimes can be located (after Legget[16]) from the requirement that the chemical potential in the superconducting phase reach the bottom of the electronic band, i.e., from $\mu_S=-W/2$. In the SBMFA μ_S is given by

$$\frac{1}{N}\frac{\partial F^S}{\partial n}=\frac{1}{N}\frac{\partial F_f}{\partial q_S}\frac{\partial q_S}{\partial n}-\frac{|U|}{2}-\lambda_1-\mu_S=0 \tag{32}$$

and determined together with the stability conditions [Eqs. (24)–(28)]. The borderline is shown in Fig. 5 as a function of n. The dashed curve in Fig. 5 represents the borderline obtained in the HFA,[17] which for the rectangular density of states (DOS) is determined by

$$\mu_S^{\rm HF}=(n-1)\frac{W}{2}\coth\left(\frac{W}{|U|}\right)-|U|n/2=-W/2.$$

As we see with increasing deviation from half-filling the boundary is shifted towards lower values of $|U|$. Let us observe that an analogous shift exhibits also the position of the maximum of the condensation energy $|\Delta F|$, which can be thought of as another indication of the crossover between the region of weakly and strongly coupled electrons. The corresponding plot is presented in Fig. 6.

III. ELECTROMAGNETIC PROPERTIES

The coupling of electrons to the external magnetic field may be expressed by a change of the phase

$$\Phi_{ij}=-\frac{e}{\hbar c}\int_{\mathbf{R}_i}^{\mathbf{R}_j}d\mathbf{r}\mathbf{A}(\mathbf{r})$$

of electrons hopping between the sites i and j. The $\mathbf{A}(\mathbf{r})$ is the vector potential of the magnetic field in the Peierls scaling, and e is the charge of an electron. It modifies the Hubbard Hamiltonian (14):

$$H=t\sum_{ij,\sigma}{}' \ (e^{i\Phi_{ij}}c^{\dagger}_{i\sigma}c_{j\sigma}+\text{H.c.})-\mu\sum_{i\sigma} \ c^{\dagger}_{i\sigma}c_{i\sigma}$$

$$-|U|\sum_{i} \ n_{i+}n_{i-}. \tag{33}$$

The current operator may be obtained by differentiation of H [Eq. (33)] with respect to the vector potential $\mathbf{A}$. In the linear approximation we get the current operator as a sum of the diamagnetic and paramagnetic parts,

$$j_{\alpha}(i)=j^{\text{dia}}_{\alpha}(i)+j^{\text{para}}_{\alpha}(i)=e^2A_{\alpha}(i)t\sum_{\sigma} \ (c^{\dagger}_{i\sigma}c_{i+a_{\alpha}\sigma}+\text{H.c.})$$

$$+iet\sum_{\sigma} \ (c^{\dagger}_{i\sigma}c_{i+a_{\alpha}\sigma}-\text{H.c.}) \tag{34}$$

($\alpha=x,y,z$). From the linear response theory[18,19] the expectation value of the Fourier transform of the total current operator is

$$J_{\alpha}(\mathbf{q},\omega)=N\frac{c}{4\pi}\sum_{\beta} \ [\delta_{\alpha\beta}K^{\text{dia}}_{\alpha}+K^{\text{para}}_{\alpha\beta}(\mathbf{q},\omega)]A_{\beta}(\mathbf{q},\omega). \tag{35}$$

The diamagnetic contribution is

$$K^{\text{dia}}_{\alpha}=\frac{8\pi e^2}{\hbar^2c^2a}\frac{t}{N}\sum_{k_{\alpha}\sigma}\langle c^{\dagger}_{k_{\alpha}\sigma}c_{k_{\alpha}\sigma}\rangle\cos(k_{\alpha}a). \tag{36}$$

The paramagnetic part is expressed by the retarded current-current Green's function

$$K^{\text{para}}_{\alpha\beta}(\mathbf{q},\omega)=\frac{4\pi}{c^2}\frac{i}{N}\int_{-\infty}^{\infty}dte^{-i\omega t}\theta(t)\langle[j^{\text{para}}_{\alpha}(\mathbf{q},t),j^{\text{para}}_{\beta}(-\mathbf{q})]\rangle, \tag{37}$$

where $j^{\text{para}}_{\alpha}(\mathbf{q},t)$ is the space-Fourier transform of the paramagnetic part of the current operator [Eq. (34)] in the Heisenberg representation. In the London superconductors the magnetic field penetration depth λ is determined by the transverse part of the total kernel in the static limit:

$$\lambda=[-K^{\text{dia}}-\lim_{q_y\to 0}K^{\text{para}}(q_x=0,q_y,q_z;\omega=0)]^{-1/2}. \tag{38}$$

At the temperature $T=0$ the paramagnetic part of the kernel may be important in determining λ. It happens in the case of nonlocal (Pippard) superconductors when the correlation length becomes greater than the penetration depth λ. This situation is common in many low-T_c systems. The short-coherence-length superconductors represent the opposite, i.e., the London limit. In the latter case the ground-state penetration depth is determined entirely by the $\mathbf{q}\to 0$ limit of the kernel where the paramagnetic part of the kernel vanishes and λ is given by

$$\lambda=\frac{1}{\sqrt{-K^{\text{dia}}}}. \tag{39}$$

In the SBMFA the diamagnetic part of the kernel K is given by

$$K^{\text{dia}}_{\alpha}=\frac{8\pi e^2}{\hbar^2c^2a}\frac{t}{N}\sum_{i_{\alpha}j_{\alpha}}{}' \ \sum_{\sigma'\sigma''}[\langle q_{i_{\alpha}j_{\alpha},\sigma'\sigma''}\rangle\langle f^{\dagger}_{i_{\alpha}\sigma'}f_{j_{\alpha}\sigma''}\rangle$$

$$+\langle r_{i_{\alpha}j_{\alpha},\sigma'\sigma''}\rangle\langle f_{i_{\alpha}-\sigma'}f_{j_{\alpha}\sigma''}\rangle+\text{c.c.}]. \tag{40}$$

For hypercubic lattices one can express K^{dia}_{α} by the average value of the kinetic energy $\langle E_{\text{kin}}\rangle$ and, therefore,

$$K^{\text{dia}}=\frac{8\pi e^2}{\hbar^2c^2a}\frac{\langle E_{\text{kin}}\rangle}{zN}=\frac{8\pi e^2}{\hbar^2c^2a}\frac{q_S}{zN}\frac{\partial F}{\partial q_S}. \tag{41}$$

Here, we have used the relation $\langle E_{\text{kin}}\rangle=q_S\partial F/\partial q_S$ and z is the number of the nearest-neighbor sites ($z=2$ for a 1D chain, $z=4$ for a 2D square lattice, and $z=6$ for a simple cubic lattice). The quantity K^{dia} is determined together with the stability conditions, Eqs. (24)–(27). For comparison in the HFA the K^{dia} is given by

$$K^{\text{dia}}_{\text{HF}}=-\frac{4\pi e^2t}{\hbar^2c^2a}n(2-n)\left[\coth\frac{W}{|U|}-\frac{W}{|U|}\left(\sinh\frac{W}{|U|}\right)^{-2}\right]. \tag{42}$$

In our calculations of λ at $T=0$ we restrict ourselves to the London limit, having in mind the properties of the systems of interest, and finally determine the area in the $|U|-n$ parameters space where the local approximation may be valid. The value of the penetration depth calculated in this way is qualitatively good both in the weak- and strong-$|U|$ limits, in the latter case approaching the results of the perturbation theory, as will be shown below.

Using the value of the penetration depth and the difference of the free energy between the normal and superconducting phases one is able to determine the thermodynamic critical field H_c and the Ginzburg-Landau correlation length ξ_{GL} as

$$\frac{H_c^2(T)}{8\pi}=\frac{F^N(T)-F^S(T)}{Na^3}, \tag{43}$$

$$\xi_{\text{GL}}=\frac{\Phi_0}{2\pi\sqrt{2}\lambda H_c}, \tag{44}$$

where $\Phi_0=hc/2e$, and to obtain the estimation for the critical fields

$$H_{c1}\simeq\frac{\ln\kappa}{\kappa}H_c\sim\frac{\ln\kappa}{\lambda^2}$$

and

$$H_{c2}\simeq\frac{\Phi_0}{2\pi\xi^2_{\text{GL}}},$$

where $\kappa=\lambda/\xi_{\text{GL}}$.

The results of the slave-boson method are presented below. Figures 7(a) and 7(b) show the variation of the London penetration depth λ with $|U|$ and n. As $|U|$ increases λ evolves smoothly between two known limits: weakly interacting single-particle carriers (with λ^{-2} being proportional to the bandwidth) and tightly bound pairs (where λ^{-2} de-

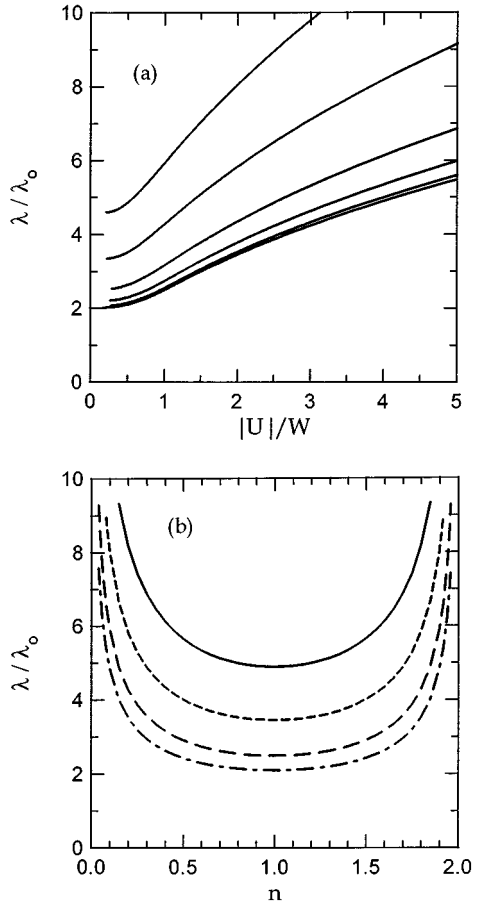

FIG. 7. The London penetration depth λ as a function of $|U|$ for $n=1$, 0.8, 0.6, 0.4, 0.2, and 0.1, from the bottom (a), and λ vs n for $|U|=4W$ (solid curve), $|U|=2W$ (short-dashed curve), $|U|=W$ (long-dashed curve), and $|U|=0.5W$ (long-short-dashed curve) (b) ($\lambda_0=(\hbar c/e)[za/8\pi W]^{1/2}$).

creases like $zt^2/|U|$). Let us notice that in the low-density limit $\lambda^{-2}\propto n^{-1/2}$ for arbitrary $|U|$. For the rectangular DOS the concentration dependence of λ is almost the same in the both limits [$\lambda^{-2}\propto n(2-n)$]. In general, for other forms of DOS it cannot be the case and in the weak-coupling limit, where the effects of DOS are most clearly seen, the n dependence of λ can strongly deviate from that one for large $|U|$ (e.g., for a fcc lattice the maximum of λ^{-2} is shifted from $n=1$ towards $n<1$).[13] Figure 8 as well as the results of the Sec. IV shows that λ calculated by the SBMFA is rather close to that obtained by the HFA, for any $|U|$ and n, as well as to that obtained by the exact low-density expansion in the large $|U|$ limit. A more significant difference between the results of the SBMFA and HFA is seen only in the intermediate region of $|U|$, where band narrowing is relevant (q_S deviates maximally from 1).

The plot of the thermodynamic critical field H_c as a function of $|U|$ is shown in Fig. 9(a) for various electron concentrations n. With increasing $|U|$ the H_c^2 increases exponentially for small values of $|U|$, and then it goes through a round maximum and it decreases as $t^2/|U|$ for large $|U|$. The maximum is placed in the crossover regime and its position depends on the electron density. For the rectangular DOS the calculated maximum of H_c is at $|U|/W\simeq 2$ in the half-filled

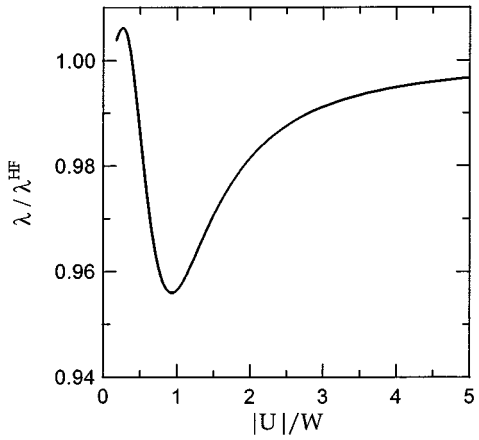

FIG. 8. Ratio of the London penetration depth calculated in the SBMFA and the HFA vs $|U|$ for $n=1$.

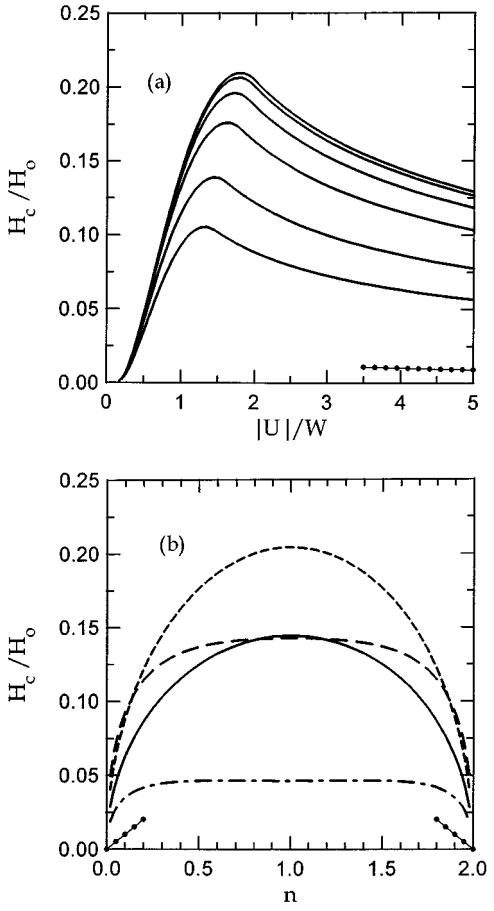

FIG. 9. Critical field H_c as a function of $|U|$ for different electron concentrations $n=1$, 0.8, 0.6, 0.4, 0.2, and 0.1 (a), and H_c vs n for $|U|=4W$ (solid curve), $|U|=2W$ (short-dashed curve), $|U|=W$ (long-dashed curve), and $|U|=0.5W$ (long-short-dashed curve) (b) ($H_0=[8\pi W/a^3]^{1/2}$). The curves with dots correspond to the exact low-density expansion results for the strong-coupling limit [Eq. (71)] calculated for the sc lattice at $n=0.1$ (a) and $|U|/W=4$ (b).

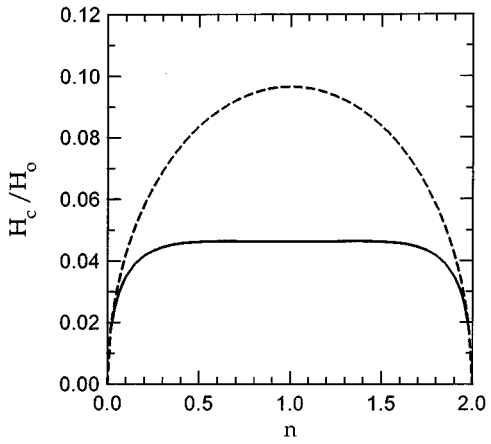

FIG. 10. Comparison of H_c obtained by the slave-boson method (solid curve) and the HF approximation for $|U|=0.5W$.

band case and with increasing $|n-1|$ it is shifted towards smaller values of $|U|/W$ (compare Figs. 5 and 6). The concentration dependences of H_c for several fixed values of $|U|$ are presented in Fig. 9(b). Let us stress that for $|U|/W<1$ the H_c remains almost constant in a quite extended region of electron concentrations, which is in contrast with the predictions of the HFA; cf. Fig. 10.

As H_c is proportional to a square root of the free energy difference between the normal and superconducting states it is a good measure of the condensation energy of the system. Taking into account that the superconducting critical temperature T_c should behave roughly as the condensation energy at $T=0$ one expects that the dependence of H_c^2 and T_c on $|U|$ and n will be qualitatively the same. The available results for T_c vs $|U|$ in the half-filled band case obtained applying Monte Carlo simulations[20,21] and the Gutzwiller-type variational approach of Hasegawa[22] are in agreement with this expectation. For arbitrary n, the only calculations of the T_c maximum have been performed until now using the effective Hamiltonian derived by the perturbation expansion in $t/|U|$ up to fifth order.[23] They show a shift of this maximum towards lower values of $|U|/W$ with decreasing n, being in agreement with our results for H_c.

In Fig. 11 we show the evolution of the Ginzburg-Landau correlation length ξ_{GL} with $|U|$ and n. With increasing $|U|$ the correlation length rapidly decreases at small $|U|$ [$\xi_{\mathrm{GL}} \propto \exp(-2|U|/W)$, for $|U| \ll W$] and tends to a constant value $a/2\sqrt{z}=\xi_\infty$, the same for all n at large $|U|$. The value of $|U|/W$ at which ξ_{GL} becomes comparable with ξ_∞ is reduced with increasing deviation from a half-filling. This can be treated as an additional indication that the crossover between the BCS and the local pair condensation regimes is shifted towards lower $|U|/W$ with decreasing n (compare Figs. 5 and 6). Let us notice a substantial variation of ξ_{GL} with n in the weak–to–intermediate-coupling regime, where ξ_{GL} attains the maximal value at half-filling. This should be contrasted with the HFA results, which for the rectangular DOS yield ξ_{GL} being n independent for any $|U|$, and predict that $\xi_{\mathrm{GL}} \to 0$ ($\xi_{\mathrm{GL}} \propto t/|U|$) if $|U|/t \to \infty$ (see Fig. 12).

Figures 13(a) and 13(b) show the plot of the Ginzburg ratio $\kappa=\lambda/\xi_{\mathrm{GL}}$. The increase of κ with $|U|$ is exponential in the weak-coupling limit [$\kappa \propto \exp(-W/|U|)$], whereas in the

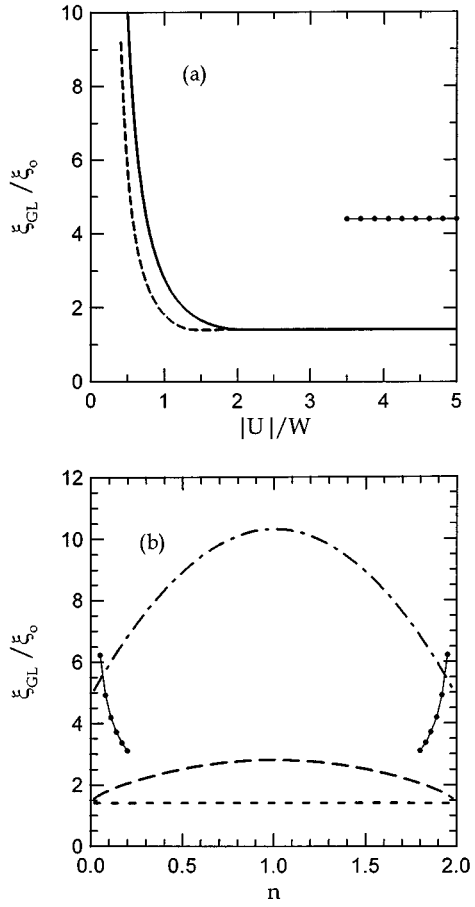

FIG. 11. The Ginzburg-Landau correlation length ξ_{GL} vs $|U|$ for $n=1$ (solid curve) and 0.1 (dashed curve) (a), and ξ_{GL} vs n for $|U|=0.5W$ (long-short-dashed curve), $|U|=W$ (long-dashed curve), and $|U|=2W$ (short-dashed curve) (b) ($\xi_0=a/[2(2z)^{1/2}]$). The curves with dots correspond to the exact low-density expansion results for the strong-coupling limit [Eq. (73)] calculated for the sc lattice at $n=0.1$ (a) and arbitrary $|U| \gg W$ (b).

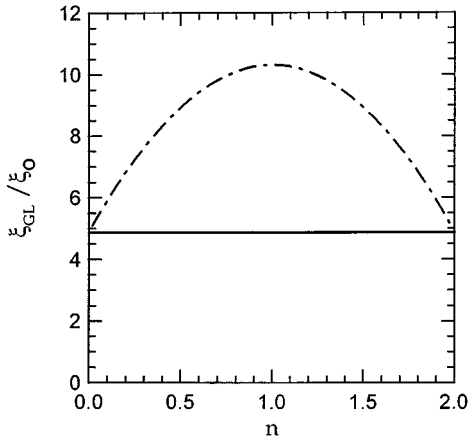

FIG. 12. Comparison of ξ_{GL} determined by the SBMFA (long-short-dashed curve) with that calculated in the HFA for $|U|=0.5W$.

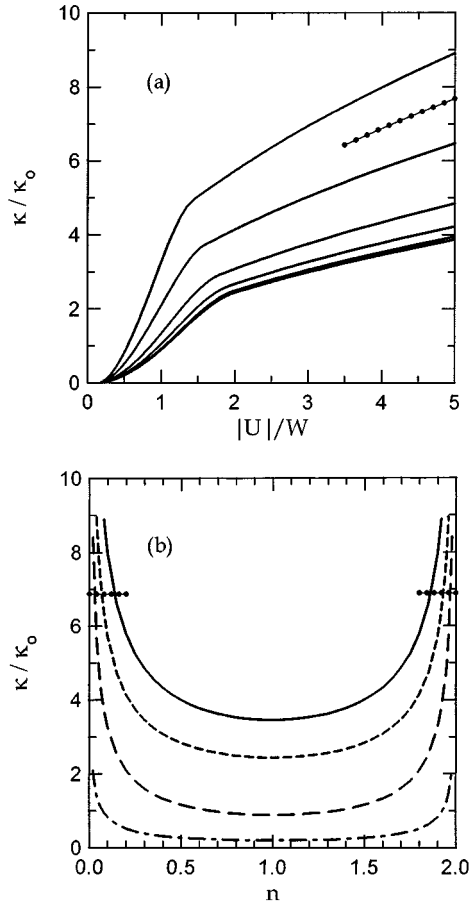

FIG. 13. The Ginzburg ratio $\kappa=\lambda/\xi_{\mathrm{GL}}$ vs $|U|$ for $n=1$, 0.8, 0.6, 0.4, 0.2, and 0.1, from the bottom (a), and κ vs n for $|U|=4W$ (solid curve), $|U|=2W$ (short-dashed curve), $|U|=W$ (long-dashed curve), and $|U|=0.5W$ (long-short-dashed curve) (b) ($\kappa_0=(\hbar c/e)z/[\pi aW]^{1/2}$). The curves with dots correspond to the exact low-density expansion results for the strong-coupling limit [Eq. (74)] calculated for the sc lattice at $n=0.1$ (a) and $|U|/W=4$ (b).

opposite limit κ becomes proportional to $\sqrt{|U|/t^2}$ (see Sec. IV). A crossover between these two types of behavior takes place for intermediate values of $|U|$ ($1<|U|/W<2$). Notice the universal κ vs n dependences: (i) $\kappa\propto 1/\sqrt{n}$ for $n\ll 1$ (arbitrary $|U|$) and (ii) $\kappa\propto 1/\sqrt{n(2-n)}$ for $|U|\gg W$. As we see from Fig. 13(b) the HFA can strongly overestimate the κ value, even in the weak-coupling regime (see the discussion on the ratio γ in Sec. IV and Appendix B).

From the equation $\kappa=1/\sqrt{2}$ one can estimate the boundaries between the local and nonlocal electromagnetic behaviors in the considered system. In Table I we have given examples of such estimations of $|U|/W$ for two fixed (t,a) values and $n=1$, 0.1 (which can be reliable for $Ba_{1-x}K_xBiO_3$ and K_xC_{60}). In the low-concentration limit, where $\kappa\propto 1/\sqrt{n}$, the local electromagnetic behavior can extend up to very small values of $|U|/W$. Notice that κ depends on the material parameters a and t in a universal way: $\kappa\propto 1/\sqrt{at}$ and for any fixed $|U|/W$ and n the Ginzburg ratio κ increases with decreasing at.

TABLE I. The values of $|U|$ (in eV) providing $\kappa=1/\sqrt{2}$ and 100 calculated for two sets of the hopping integral and the lattice constant (t,a), which approximately correspond for $Ba_{1-x}K_xBiO_3$ and K_xC_{60}, respectively.

		$t=0.1$ eV $a=4$ Å	$t=0.1$ eV $a=14$ Å
$\kappa=1/\sqrt{2}$	$n=1$	0.16	0.18
	$n=0.1$	0.14	0.15
$\kappa=100$	$n=1$	0.49	0.63
	$n=0.1$	0.32	0.38

IV. RESULTS FOR $|U|\gg W$ OBTAINED USING THE EFFECTIVE PSEUDOSPIN MODEL AND THEIR COMPARISON WITH THE SBMFA

For $|U|\gg W$ we can resort to the perturbation theory in an analysis of the Hubbard model with the attractive interaction. In this limit a large gap E_g of order $|U|$ exists in the single-particle spectrum for any n [cf. Figs. 4(a) and 5(a)], which is equivalent to the statement that the Fermi level is pinned close to $-|U|/2$. Due to that fact, the standard degenerate perturbation theory can be applied for the model (14) and (33) to derive the effective pseudospin Hamiltonian valid for any band filling, working in the subspace excluding the single occupancy of sites. Up to second order in a small parameter $t/|U|$ one obtains[1,14,23]

$$\widetilde{H}=-\frac{J}{2}{\sum_{ij}}'\ (e^{2i\Phi_{ij}}\rho_i^+\rho_j^-+\mathrm{H.c.})$$

$$+J{\sum_{ij}}'\ \rho_i^z\rho_j^z-\overline{\mu}\sum_i\ (2\rho_i^z+1)-\frac{N}{4}zJ, \qquad (45)$$

where $2\rho_i^z=(n_{i+}+n_{i-}-1)$, $\rho_i^+=c_{i+}^\dagger c_{i-}^\dagger$, $J=2t^2/|U|$, and $\overline{\mu}=\mu+|U|/2$. The operators: $\rho_i^\pm$ and ρ_j^z are the charge operators, which in the subspace excluding single occupancy of sites satisfy the commutation rules of the $s=1/2$ operators. The electron number condition is

$$n=\frac{1}{N}\sum_i\ \langle 2\rho_i^z+1\rangle. \qquad (46)$$

For $\langle\rho^+\rangle=(1/N)\Sigma_i\langle\rho_i^+\rangle\neq 0$ the Hamiltonian (45) describes the superconducting state.

It is worthwhile to compare the strong-coupling results of the SBMFA approach with the ones obtained for Eq. (45). Recently the thermodynamic and electromagnetic properties of the model (45) have been analyzed in Refs. 24 and 25 and below we only quote the final expressions for the ground-state characteristics derived within the MFA. [The random phase approximation (RPA) treatment, taking into account quantum corrections, yields for 3D lattices qualitatively similar results, except for the low-concentration limit.[25] Notice also that for the model (45) the MFA treatment becomes an exact theory in the limit of an infinite number of spatial dimensions $D=\infty$.] The MFA calculations of the free energy at $T=0$ (the ground-state energy) for the superconducting and the normal ($\langle\rho^+\rangle=0$) states give[13,14,24,25]

$$F^S/N=-\frac{|U|}{2}n-z\frac{t^2}{|U|}n(2-n), \qquad (47)$$

$$F^N/N=-\frac{|U|}{2}n-\frac{1}{2}z\frac{t^2}{|U|}n(2-n), \tag{48}$$

$$\Delta=\langle\rho^+\rangle=\frac{1}{2}\sqrt{n(2-n)}, \tag{49}$$

$$\mu_S=-\frac{|U|}{2}-z\frac{t^2}{|U|}(2-2n), \tag{50}$$

and the electromagnetic quantities H_c, λ, ξ_{GL}, and κ are

$$\frac{H_c^2}{8\pi}=\frac{zn(2-n)}{2a^3}\frac{t^2}{|U|}, \tag{51}$$

$$\lambda^{-2}=\frac{16\pi e^2 n(2-n)}{\hbar^2 c^2 a}\frac{t^2}{|U|}, \tag{52}$$

$$\xi_{\mathrm{GL}}=\frac{a}{\sqrt{2z}}, \tag{53}$$

$$\kappa=\frac{\hbar c}{e}\frac{\sqrt{z}}{\sqrt{2\pi a n(2-n)t^2/|U|}}. \tag{54}$$

For comparison with Eqs. (47)–(54) we have performed a strong-coupling expansion of the set of equations (24)–(28) describing the superconducting phase within the SBMFA, up to second order in $t/|U|$. A recent analogous expansion for the energy of the antiferromagnetic phase of the half-filled repulsive Hubbard model has been derived by Denteneer[26] up to fifth order in t/U. The expansion can be obtained in terms of moments of the density of states for the hypercubic lattices in an arbitrary dimension and the final results for the quantities of interest obtained in this way are the following:

$$F^S/N=-\frac{|U|}{2}n-M_2\frac{t^2}{|U|}n(2-n), \tag{55}$$

$$F^N/N=-\frac{|U|}{2}n, \tag{56}$$

$$\Delta=\frac{1}{2}\sqrt{n(2-n)}\left[1-2M_2\left(\frac{t}{|U|}\right)^2\right], \tag{57}$$

$$\mu_S=-\frac{|U|}{2}+M_2\frac{t^2}{|U|}(2-2n), \tag{58}$$

$$E_g=|U|\left[1-2M_2\frac{t}{|U|}\left|n-1\right|+O\left(\frac{t^2}{|U|^2}\right)\right], \tag{59}$$

$$\frac{H_c^2}{8\pi}=\frac{M_2 n(2-n)}{a^3}\frac{t^2}{|U|}, \tag{60}$$

$$\lambda^{-2}=\frac{16\pi e^2 n(2-n)}{\hbar^2 c^2 a}\frac{t^2}{|U|}, \tag{61}$$

$$\xi_{\mathrm{GL}}=\frac{a}{2\sqrt{M_2}}, \tag{62}$$

$$\kappa=\frac{\hbar c}{e}\frac{\sqrt{M_2}}{\sqrt{\pi a n(2-n)t^2/|U|}}, \tag{63}$$

where $M_2=z=2D$ is the second moment of the density of states for a D-dimensional hypercubic lattice. As we see the results for F^S, μ_S, and λ are identical in both approaches. Expressions (51) and (60) for H_c^2 differ by a factor of 2, whereas Eqs. (53) and (62) (for ξ_{GL}) as well as Eqs. (54) and (63) (for κ) by a factor $1/\sqrt{2}$ and $\sqrt{2}$, respectively. This is due to overestimation of F^N by the SBMFA for large $|U|$ [compare Eqs. (48) and (56)]—this approximation, being equivalent to the Gutzwiller approximation, neglects entirely the intersite correlations in the normal phase. The consequences of this shortcoming are most drastic in the low-density limit, which we will conclude in the following.

The effective pseudospin model (45) can be equivalently treated as a model of bosons on a lattice with infinite on-site repulsion (hard core) and with the nearest-neighbor (NN) hopping integral equal to the NN density-density interaction. It is clearly seen by the representation

$$\rho_i^-=b_i, \quad \rho_i^+=b_i^\dagger, \quad \rho_i^z=-\frac{1}{2}+b_i^\dagger b_i, \tag{64}$$

which transforms Eqs. (45) and (46) into

$$\widetilde{H}=-\frac{J}{2}{\sum_{ij}}' \ (e^{2i\Phi_{ij}}b_i^\dagger b_j+\mathrm{H.c.})+J{\sum_{ij}}' \ n_i n_j-\widetilde{\mu}\sum_i \ n_i, \tag{65}$$

$$\overline{n}=n/2=\frac{1}{N}\sum_i \ \langle n_i\rangle, \tag{66}$$

where $n_i=b_i^\dagger b_i$ and $\widetilde{\mu}=2\overline{\mu}+zJ$. The hard-core boson operators b_i satisfy the Pauli commutation relations

$$[b_i^\dagger,b_j]=(2n_i-1)\delta_{ij}, \quad (b_i^\dagger)^2=b_i^2=0, \quad b_i^\dagger b_i+b_i b_i^\dagger=1, \tag{67}$$

which exclude multiple boson occupancy of a given site, and the number of bosons per site $\overline{n}=n/2$ is given by Eq. (66), which determines the chemical potential $\widetilde{\mu}$. Recently, several rigorous results concerning the ground-state properties of the model of hard-core charged bosons, Eq. (64), on a lattice have been derived for various 3D lattices, using a systematic low-density expansion based on the knowledge of exact two-body scattering amplitude.[25] Transforming the results of Ref. 25 (Sec.VI B) into our problem one gets for $n\to 0$ the following exact expressions [for simplicity we present only the leading terms of expansions, crucial for comparison with Eqs. (47)–(63)]:

$$F^S/N=-\frac{|U|}{2}n-z\frac{t^2}{|U|}n\left(2-\frac{1}{2}\alpha n\right)+O(n^{5/2}), \tag{68}$$

$$F^N/N=-\frac{|U|}{2}n-z\frac{t^2}{|U|}n(2-\alpha n), \tag{69}$$

$$\mu_S=-\frac{|U|}{2}-z\frac{t^2}{|U|}(2-\alpha n)+O(n^{3/2}), \tag{70}$$

$$\frac{H_c^2}{8\pi}=\frac{1}{2}\alpha z\frac{t^2}{|U|}\frac{n^2}{a^3}+O(n^{5/2}), \tag{71}$$

$$\lambda^{-2}=\frac{4\pi e^2}{\hbar^2 c^2 a}\frac{t^2}{|U|}\{n(2-n)+n^2(C-1)[2\alpha+\alpha^2(2C-3)+O(n^{5/2})]\}, \tag{72}$$

$$\xi_{\mathrm{GL}}=\frac{a}{\sqrt{2z}}\frac{1}{\sqrt{\alpha[n+O(n^2)]}}, \tag{73}$$

$$\kappa=\frac{\hbar c}{2e}\frac{\sqrt{z\alpha}}{\sqrt{2\pi a t^2/|U|}}, \tag{74}$$

where $\alpha=2/(2C-1)$ is the exact two-particle scattering amplitude for the model (45) ($\alpha=0.9839$, 1.1196, and 1.1840 for sc, bcc, and fcc lattices, respectively) and C is the Watson integral for a given lattice [$C=(1/N)\Sigma_k(1-\epsilon_k/\epsilon_0)^{-1}$, and $C=$ 1.5164 (sc), 1.3932 (bcc), and 1.3446 (fcc)]. As we see, the terms up to order $(t^2/|U|)n$ in the expansions of F^S and λ^{-2} are correctly given by the SBMFA, whereas in F^N only the first term $[-(|U|/2)n]$ is correct. The overestimation of F^N by the terms of order $(zt^2/|U|)n$ results in erroneous n dependences of H_c, ξ, and κ in the both previously discussed approximations. Comparison of Eqs. (71), (74), and (73) with (60), (63), and (62) shows that for $n\to 0$ the correct values of H_c and κ can be much smaller and that of ξ_{GL}, much larger than those predicted by the SBMFA. These differences are clearly seen in Figs. 9, 13, and 11, where the exact results [Eqs. (71), (74), and (73)] are given by curves with dots.

V. DISCUSSION AND FINAL REMARKS

Our analysis of the attractive Hubbard model by the SBMFA has shown that in the weak-coupling limit the gap E_g in the excitation spectrum at $T=0$ is reduced in comparison to that obtained in the HFA by a renormalization factor γ ($E_g=\gamma E_g^{\mathrm{HF}}$). The renormalizations concern most of the other superfluid characteristics of the system (see Appendix B), the thermodynamical magnetic field [$H_c=(\gamma/\sqrt{q_S})H_c^{\mathrm{HF}}$], the coherence length [$\xi_{\mathrm{GL}}=(q_S/\gamma)\xi_{\mathrm{GL}}^{\mathrm{HF}}$], and the Ginzburg ratio [$\kappa=(\gamma/q_S^{3/2})\kappa^{\mathrm{HF}}$], and only the London penetration depth remains almost unrenormalized [$\lambda=(1/q_S)\lambda^{\mathrm{HF}}$; $q_S\to 1$ if $|U|\to 0$]. The value of γ is found to be a function of the electron concentration n. The renormalization is maximal in the half-filled band case and it is reduced with increasing $|n-1|$ [cf. Fig. 4(b), $\gamma\to 1$ for $n\to 0$].

Recently the half-filled Hubbard model has been extensively considered at weak coupling within the self-consistent second-order $t/U\ll 1$ perturbation treatment taking into account the vertex corrections (see Ref. 27 for $U>0$ and Ref. 28 for $U<0$; notice that for $n=1$ the repulsive Hubbard model can be mapped to the negative U model by the *repulsion-attraction* transformation[1,14]). These analyses show a decrease of the gap parameter and the critical temperature T_c with respect to the HFA solution by the same renormalization factor γ [such that the ratio $E_g(T=0)/k_BT_c$ for $U\to 0$ is identical to the BCS ratio 3.5285 found in the HFA (Ref. 27)] and in the case of a D-dimensional hypercubic lattice the value of γ has been estimated to be $\gamma\simeq 0.288-0.016/D$, for $|U|\to 0$.[27] A similar renormalization in the weak-coupling limit ($\gamma\simeq 0.4$) has been also found by Jarrell,[21] who calculated T_c using numerical Monte Carlo simulations for the Hubbard model in infinite dimensions. Both these results are in agreement with our SBMFA calculations, performed using a rectangular DOS, which for $|U|\to 0$, $n=1$ predict $\gamma\simeq 0.47$.

The attractive Hubbard model is probably the simplest lattice model to display a crossover from BCS-like to local pair (composite bosons) superconductivity. The previous analyses of the crossover have been performed using (broken symmetry) HFA. They have shown the smooth evolution of the ground-state energy and the single-particle excitations in the superconducting phase from weak to strong coupling.[1,15] More recent studies of the collective excitations performed within the HFA RPA have also found a continuous evolution of the collective-mode spectrum from the Anderson mode, for weak coupling, into the Bogoliubov sound mode for hard-core bosons.[17,29] In the present work we have studied the basic (ground-state) superfluid characteristics of the $U<0$ model going beyond the HFA. We have found that the SBMFA (in contrast to the HFA) gives credible results for all the investigated quantities in the whole interaction range interpolating smoothly between the weak- and strong-coupling regimes, where it matches well the results of the perturbation methods developed for these limits. The values of the calculated ground-state energy of the superconducting phase, the chemical potential, and the London penetration depth are quite close to those obtained within the HFA for any $|U|$ and n. The largest differences, but not higher than 5%, are found near half-filling in the intermediate-coupling regime $|U|/W\approx 1$. On the other hand, we have shown that although the HFA predictions for the behavior of the energy gap vs $|U|$ are qualitatively satisfactory, quantitatively they can be off by a factor of 2–3 for $0<|U|/W<1$. Moreover, we have found that for several superfluid properties (ξ_{GL}, H_c, κ) the validity of the HFA is restricted to the case of low electron concentrations in the $|U|/W\ll 1$ limit only, and that beyond this regime it gives erroneous behavior of these quantities. This failure is due to the fact that the HFA greatly overestimates the free energy of the normal state, which is used in a standard calculation of H_c and next ξ_{GL}.

As follows from Sec. IV the attractive Hubbard model in the large $|U|$ limit ($|U|\gg W$, k_BT) can be equivalently considered either as the pseudospin Heisenberg model with a fixed magnetization [Eqs. (45) and (46)] or as the model of hard-core bosons with a charge $2e$ and the hopping integral equal to the intersite density interaction [Eqs. (65) and (66)]. For these equivalent models we have presented (in Sec. IV) the results derived within the MFA (for arbitrary n) as well as the rigorous results obtained using a systematic low-density expansion ($n\ll 1$) for various 3D lattices. The MFA results [which for the models (45) and (65) become the exact ones in the $D\to\infty$ limit] are found to be very close to the strong-coupling results of the SBMFA for any concentration of electrons. For $n\ll 1$ the comparison with rigorous low-density expansion results for 3D lattices shows that in the limit $|U|/W\gg 1$ F^S, μ_S and λ^{-2} are correctly given by the SBMFA [up to the order $(t^2/|U|)n$], whereas F^N and, con-

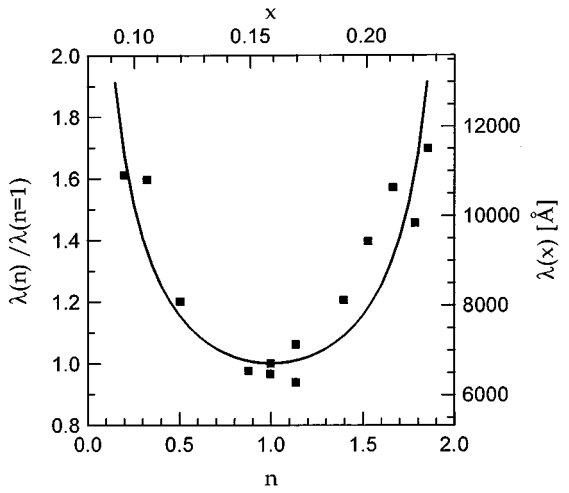

FIG. 14. The London penetration depth λ normalized to its value at $n=1$ (left axis) as a function of the electron concentration n (lower axis) obtained for the attractive Hubbard model in SBMFA for $|U|/W=0.4$, and experimental results (Ref. 34) (squares) for $La_{2-x}Sr_xCuO_4$ films (right and upper axis).

sequently, H_c are substantially overestimated by this approach.

Although our model seems to be oversimplified for quantitative relations with experiment, nevertheless some of the theoretical predictions should be experimentally testable, at least on a qualitative level. Among the recently studied superconducting materials the best candidates for such comparisons are the extreme type-II superconductors. This group of materials, including the cuprates, fullerides, Chevrel phases, and bismuthates, generally exhibits several unique features such as high T_c at relatively low carrier density, small value of the Fermi energy, $\sim$ 0.1–0.3 eV, short coherence length (which can be of order of interparticle distance or even a lattice constant), extremely large λ/ξ_{GL} ratio, and the universal trends in the T_c versus condensate density dependence (universal dependence $T_c/T_c^{\max}$ vs $[\lambda(0)/\lambda(0)^{\max}]^2$).[1,30–33] Moreover, they have T_c proportional to T_F (the Fermi temperature) or T_B (the Bose-Einstein condensation temperature), with $T_B \simeq (3-30)T_c$ and $T_F \simeq (10-100)T_c$.[30] All these features clearly support the models with short-range, nonretarded attraction (see Ref. 1 for review). For all above superconductors the experimentally estimated Ginzburg ratio is of order 100.[30–33] Thus, from the equality $\kappa=100$ one can estimate the values of $|U|/W$ and n, which eventually could be reliable for these materials. Examples of such estimations are given in Table I and they indicate that the best agreement can be obtained for intermediate values of the local attraction. An important test for the theory would be the measurements of λ, H_c, and ξ_{GL} as a function of electron concentration n. Very recently Locquet *et al.*[34] have reported penetration depth measurements for $La_{2-x}Sr_xCuO_4$ films as a function of doping, extending in the range from heavily underdoped to heavily overdoped. As it follows from Fig. 14 the theoretical plots of $\lambda(n)/\lambda(n=1)$ for our simple model fit surprisingly well these experimental data. With respect to the Ginzburg-Landau coherence length ξ_{GL} the theory predicts its relatively weak density dependence (a slow increase with n) in the intermediate-coupling regimes [compare Fig. 11(b)]. Experimental results on ξ_{GL} in the cuprates seem to confirm this prediction. The in-plane ξ_{GL} is found to be almost density independent, and the out-of-plane ξ_{GL} to increase with n.[35] Unfortunately, we are not aware of existing analogous experimental data for other families of nonconventional superconductors (the measurements for doped bismuthates would be most interesting in this respect).

The slave-boson mean-field approach (SBMFA) seems to be, at present, the only systematic and simple method which takes into account correlations of electrons and yields reliable description of all superfluid characteristics of the attractive Hubbard model for any electron concentration and arbitrary $|U|$. Moreover, the method can be easily extended to study more general models, including intersite interaction terms like the correlated hopping, the Coulomb interactions, and the intersite charge and spin exchange, as well as the electron-phonon coupling, and to study the interplay between various types of superconductivity (s, p, and d type), magnetic orderings, and the charge density waves (CDW's). The present method is a mean-field type, and therefore it does not includes fluctuations of bosonic fields. We also confined our studies to the case $T=0$. However, one can use the path integral approach and extend these studies for $T>0$, taking into account fluctuations in a coherent potential approximation (CPA) (in an analogous way as one treats static[22] or dynamic fluctuations[36] for $D=\infty$).

ACKNOWLEDGMENTS

We would like to thank R. Micnas, T. Kostyrko, and P. van Dongen for many useful discussions. We are grateful for the financial support by the Polish Research Committee of Sciences within the projects 2 P03B 165 10 (B.R.B. and S.R.) and 2 P03B 104 11 (S.R.) and by the Institute for Scientific Interchange Foundation in Torino (EC PECO Network ERBCIPDCT940027).

APPENDIX A: SBMFA SOLUTIONS FOR THE NORMAL STATE

The free energy of the normal state at $T=0$ is given for the rectangular DOS by Eqs. (28) and (23) with $\Delta=0$

$$F^N/N=(F_f^N+F_b^N)/N$$
$$=-\frac{q_N W}{4}(1-\overline{\lambda_1})^2+\frac{U}{2}(b^2+2\delta)-\mu(1+2\delta), \quad \text{(A1)}$$

where the band narrowing factor $q_N=2(1-b^2)(b^2+\sqrt{b^4-4\delta^2})/(1-4\delta^2)$. (Here, the parameter U may be positive as well as negative.) The stable solutions are given in a parametric way as a function of the double-occupancy parameter $2|\delta| \leq b^2 \leq 1$. The interaction U is expressed by

$$U=W\left[1-2b^2-\frac{2b^4-b^2-4\delta^2}{\sqrt{b^4-4\delta^2}}\right], \quad \text{(A2)}$$

the free energy is

$$F^N/N=-\frac{W}{4}q_N n(2-n)+\frac{U}{2}(b^2+2\delta), \tag{A3}$$

and the chemical potential is given by

$$\mu=\frac{W}{2}\left[1-2b^2-\frac{2b^4-b^2(1-2\delta)-2\delta(1+2\delta)}{\sqrt{b^4-4\delta^2}}\right]. \tag{A4}$$

Here, $n=1+2\delta$. It is seen that for $U<0$ the width of the band is reduced to zero ($q_N=0$) at $U_c/W=[-1-\sqrt{n(2-n)}]$ (see Fig. 6). For $U<U_c$ $b^2=1$ and $F^N/N=Un/2$. The values of $U_c/(8t)$ calculated for hypercubic 1D, 2D, and 3D lattices at $n=1$ are -1.273, -1.621, and -2.005, respectively.[8] For a more detailed analysis of the normal-state solutions of the attractive Hubbard model performed using the Gutzwiller approximation to the Gutzwiller wave function (which is equivalent to our treatment of this state) we refer the reader to Ref. 37.

APPENDIX B: ANALYTICAL SBMFA RESULTS FOR $|U|/W\to 0$

Here, we want to calculate analytically the gap in the excitation spectrum and the other ground-state characteristics in the limit $|U|\to 0$ and for $n=1$, and compare them with the corresponding HF results. In the SBMFA the gap for $|U|\to 0$ is $E_g=2\lambda_S$. From Eqs. (25) and (27) we get

$$\lambda_S=|U|\Delta y, \tag{B1}$$

where

$$y=\frac{\partial q_S/\partial\Delta^2}{2\partial q_S/\partial b^2}. \tag{B2}$$

For $\lambda_S\to 0$ we find from Eqs. (26) and (28)

$$\Delta=-\frac{\overline{\lambda_S}}{2}\ln\frac{2}{\lambda_S} \tag{B3}$$

($\overline{\lambda_S}=2\lambda_S/q_S W$). Putting Eq. (B1) into Eq. (B3) we get the gap in the SBMFA:

$$E_g=2q_S W\exp\left[\frac{2q_s W}{|U|y}\right]. \tag{B4}$$

In the HFA [Eq. (31)]

$$E_g^{\mathrm{HF}}=2W\exp\left[-\frac{2W}{|U|}\right], \tag{B5}$$

and thus, the reduction parameter is given by

$$\gamma\equiv\frac{E_g}{E_g^{\mathrm{HF}}}=q_S\exp\left[\frac{2W}{|U|}\left(\frac{q_S}{y}+1\right)\right]. \tag{B6}$$

In the limit $\Delta\to 0$, $q_S\simeq 4b^2(1-b^2)$, $\partial q_S/\partial b^2\simeq 4(1-2b^2)$, and $\partial q_S/\partial\Delta^2\simeq q_S(4-1/b^4)$. From Eqs. (21), (25), and (28) we find that $q_S/y\simeq -1-3|U|/8W$ for $|U|/W\ll 1$, and therefore

$$\gamma=\exp(-3/4). \tag{B7}$$

Expansion of F^S [Eq. (28)] and F^N [Eq. (A1)] for $|U|\to 0$ yields

$$\Delta F/N=(F^N-F^S)/N=\frac{E_g^2}{8q_S W}, \tag{B8}$$

whereas the corresponding expansions of Eqs. (29) and (30) give

$$\Delta F_{\mathrm{HF}}/N=(F^N_{\mathrm{HF}}-F^S_{\mathrm{HF}})/N=\frac{(E_g^{\mathrm{HF}})^2}{8W}. \tag{B9}$$

Taking into account Eqs. (B4) and (B5) one obtains

$$\frac{\Delta F}{\Delta F_{\mathrm{HF}}}=\left(\frac{H_c}{H_c^{\mathrm{HF}}}\right)^2=\frac{\gamma^2}{q_S}. \tag{B10}$$

Analogous calculations for $1/\lambda^2$ [Eqs. (41) and (42)] give

$$\left(\frac{\lambda}{\lambda^{\mathrm{HF}}}\right)^2=\frac{1}{q_S}, \tag{B11}$$

and from Eqs. (43), (44) and (B10), (B11) it follows directly that

$$\left(\frac{\xi_{\mathrm{GL}}}{\xi_{\mathrm{GL}}^{\mathrm{HF}}}\right)^2=\left(\frac{\Delta F}{\Delta F_{\mathrm{HF}}}\right)\left(\frac{\lambda^{\mathrm{HF}}}{\lambda}\right)^2=\frac{q_S^2}{\gamma^2}, \tag{B12}$$

$$\frac{\kappa}{\kappa^{\mathrm{HF}}}=\left(\frac{\lambda}{\lambda^{\mathrm{HF}}}\right)\left(\frac{\xi^{\mathrm{HF}}}{\xi}\right)=\frac{\gamma}{q_S^{3/2}}. \tag{B13}$$

*Electronic address: bulka@ifmpan.poznan.pl
†Electronic address: saro@phys.amu.edu.pl

[1] R. Micnas, J. Ranninger, and S. Robaszkiewicz, Rev. Mod. Phys. **62**, 113 (1990).
[2] J.A. Wilson, J. Phys. C **20**, L911 (1987); **21**, 2067 (1988); Physica C **233**, 322 (1994).
[3] T.J. Schneider, H. Beck, D. Bormann, T. Meintrup, S. Schafroth, and A. Schmidt, Physica C **216**, 432 (1993).
[4] A. Taraphader, H.R. Krishnamurthy, R. Pandit, and T.V. Ramakrishnan, Phys. Rev. B **52**, 1368 (1995); Europhys. Lett. **21**, 79 (1993); C.M. Varma, Phys. Rev. Lett. **61**, 2731 (1989).
[5] S.K. Sarker, Phys. Rev. B **49**, 12 047 (1994); F.C. Zhang, M. Ogata, and T.M. Rice, Phys. Rev. Lett. **67**, 3452 (1991); S. Chakravarty and S. Kivelson, Europhys. Lett. **16**, 751 (1991); S. Chakravarty, M.P. Gelfand, and S. Kivelson, Science **254**, 970 (1991); J.A. Wilson, Physica C **182**, 1 (1991).
[6] G. Kotliar and A.E. Ruckenstein, Phys. Rev. Lett. **57**, 1362 (1986).
[7] M. Gutzwiller, Phys. Rev. Lett. **10**, 159 (1963); Phys. Rev. **137**, A1726 (1965).
[8] H. Hasegawa, Phys. Rev. B **41**, 9168 (1990); J. Phys. Condens. Matter **1**, 9325 (1989); S.M. Evans, Europhys. Lett. **20**, 53 (1992); M. Lavagna, Phys. Rev. B **41**, 142 (1990); R. Frésard and P. Wölfle, J. Phys. Condens. Matter **4**, 3625 (1992); L. Lilly, A. Muramatsu, and W. Hanke, Phys. Rev. Lett. **57**, 1362 (1990).
[9] P.J.H. Denteneer and M. Blaaauboer, J. Phys. Condens. Matter **7**, 151 (1995); **7**, 2377 (1995).
[10] J.O. Sofo and C.A. Balseiro, Phys. Rev. B **45**, 377 (1992).
[11] B.R. Bulka, Phys. Status Solidi B **180**, 401 (1993).
[12] R. Frésard and P. Wölfle, Int. J. Mod. Phys. B **6**, 685 (1992).

[13] W. Czart, T. Kostyrko, and S. Robaszkiewicz, J. Magn. Magn. Mater. **140-144**, 2059 (1995); (unpublished).
[14] S. Robaszkiewicz, R. Micnas, and K.A. Chao, Phys. Rev. B **23**, 1447 (1981).
[15] S. Robaszkiewicz, R. Micnas, and K.A. Chao, Phys. Rev. B **24**, 4018 (1981); P. Nozieres and S. Schmitt-Rink, J. Low Temp. Phys. **59**, 195 (1985).
[16] A.J. Legget, in *Modern Trends in the Theory of Condensed Matter*, edited by A. Pekalski and J. Przystawa (Springer-Verlag, Berlin, 1980), p. 13.
[17] T. Kostyrko and R. Micnas, Phys. Rev. B **46**, 11 025 (1992); Acta Phys. Pol. A **83**, 837 (1993).
[18] A.L. Fetter and J.D. Walecka, *Quantum Theory of Many-Particle Systems* (McGraw-Hill, New York, 1991).
[19] D.J. Scalapino, S.R. White, and S. Zhang, Phys. Rev. B **47**, 7995 (1993); Phys. Rev. Lett. **68**, 2830 (1992); T. Kostyrko, R. Micnas, and K.A. Chao, Phys. Rev. B **49**, 6158 (1994).
[20] R.T. Scalettar, D.J. Scalapino, R.L. Sugar, and D. Toussaint, Phys. Rev. B **39**, 4711 (1989).
[21] M. Jarrell, Phys. Rev. Lett. **69**, 168 (1992); M. Jarrell and T. Pruschke, Z. Phys. B **90**, 187 (1993).
[22] H. Hasegawa, J. Phys. Condens. Matter **1**, 9325 (1989).
[23] J.K. Freericks, Phys. Rev. B **48**, 3881 (1993); S. Robaszkiewicz, Acta Phys. Pol. A **85**, 117 (1994).
[24] R. Micnas and S. Robaszkiewicz, Phys. Rev. B **45**, 9900 (1992).
[25] R. Micnas, S. Robaszkiewicz, and T. Kostyrko, Phys. Rev. B **52**, 6863 (1995).
[26] P.J.H. Denteneer, Phys. Rev. B **53**, 9764 (1996).
[27] P.G.J. van Dongen, Phys. Rev. Lett. **67**, 757 (1991); Phys. Rev. B **50**, 14 016 (1994); A. Martin-Rodero and F. Flores, *ibid.* **45**, 13 008 (1992).
[28] J.K. Freericks and D.J. Scalapino, Phys. Rev. B **49**, 6368 (1994); J.K. Freericks, *ibid.* **50**, 403 (1994).
[29] J.O. Sofo, C.A. Balseiro, and H.E. Castillo, Phys. Rev. B **45**, 9860 (1992); L. Belkhir and M. Randeira, *ibid.* **45**, 5085 (1992).
[30] Y.J. Uemura *et al.*, Phys. Rev. Lett. **62**, 2317 (1989); **66**, 2665 (1991); Nature **352**, 605 (1991).
[31] T. Schneider and H. Keller, Phys. Rev. Lett. **69**, 3374 (1992); Int. J. Mod. Phys. B **8**, 487 (1994).
[32] K. Holczer, O. Klein, G. Grüner, J.D. Thompson, F. Dietrich, and R.L. Whetten, Phys. Rev. Lett. **67**, 271 (1991).
[33] R. Brusetti, O. Laborole, A. Sulpice, R. Calemczuk, M. Potel, and P. Goueon, Phys. Rev. B **52**, 4481 (1995).
[34] J.P. Locquet *et al.*, (unpublished); T. Schneider, in *Polarons and Bipolarons in High-T_c Superconductors and Related Materials*, edited by W.Y. Liang, E.S. Salje, and A.S. Alexandrov (Cambridge University Press, Cambridge, England, 1995), p. 258.
[35] M. Suzuki and M. Hikita, Phys. Rev. B **44**, 249 (1991).
[36] D. Vollhardt, in *Correlated Electron Systems*, edited by V.J. Emery (World Scientific, Singapore, 1993), Vol. 8, p. 57; V. Janiš, Phys. Rev. B **40**, 11 331 (1989).
[37] G.A. Medina, J. Simonin, and M.D. Nùñez-Regueiro, Phys. Rev. B **43**, 6206 (1991).